

Hydrated area of a bentonite layer encapsulated between two geomembranes

Edit 6 2001.12.22 date to be deleted, but keep space here

J.P. GIROUD, JP GIROUD, INC., Ocean Ridge, Florida, USA

R.S. THIEL, Thiel Engineering

E. KAVAZANJIAN & F.J. LAURO, GeoSyntec Consultants, Huntington Beach, California, USA

ABSTRACT: Hydrated bentonite has low shear strength, which may adversely impact the stability of structures incorporating geosynthetic clay liners (GCLs). Accordingly, in some applications of GCLs, bentonite is encapsulated between two geomembranes to minimize hydration of the bentonite. If the lower geomembrane is overlapped instead of welded, water can migrate from the underlying ground into the bentonite, and, then, migrate laterally in the bentonite between the two geomembranes. This paper presents an analytical method to evaluate the extent of the hydrated area of the bentonite as a function of: time, the porosity and hydrated hydraulic conductivity of the bentonite, the overlap width, the distance between overlaps, and the suction potential at the hydration front. Numerical applications of the method show that, for typical values of the parameters, it takes many decades to hydrate a significant fraction of the bentonite area. [139 words, 150 authorized]

1 INTRODUCTION

1.1 Situation considered

This paper presents a theoretical evaluation of the hydrated area of a layer of bentonite encapsulated between two geomembranes, with the upper geomembrane seams welded and the lower geomembrane seams formed by overlap. This configuration is used, in particular, in applications where it is important to minimize the extent of the hydrated area of the bentonite component of a geosynthetic clay liner (GCL). This is the case in waste containment landfills where the low shear strength of hydrated bentonite may impact the stability of the landfill.

Two types of GCLs are currently available: GCLs where the bentonite layer is contained between two geotextiles, and GCLs where the bentonite layer is associated with a carrier geomembrane (hereafter designated as GM-GCLs). There are several possibilities for encapsulating a bentonite layer between two geomembranes. This paper is devoted to the case where a GM-GCL is placed first with the bentonite layer up, and a geomembrane is placed on top of the GM-GCL. It is assumed that panels of GM-GCL are simply overlapped at the seams (Figure 1). In other words, the geomembrane component of the GM-GCL is not welded.

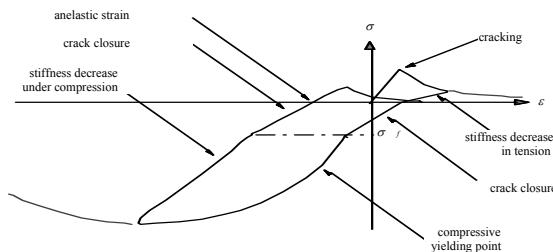


Figure 1. Schematic representation of an overlap of a GCL composed of a layer of bentonite and a geomembrane. Arrows show the direction of liquid migration.

Figure 2 illustrates the geometry of a GM-GCL panel with overlapped seams, wherein: B_o = overlap width; W_p = panel width; $W_p - B_o$ = effective panel width; L_p = panel length; and $L_p - B_o$ = effective panel length. The “width of the hydrated area”, W_H , refers to the width of the hydrated area within the effective width of a panel.

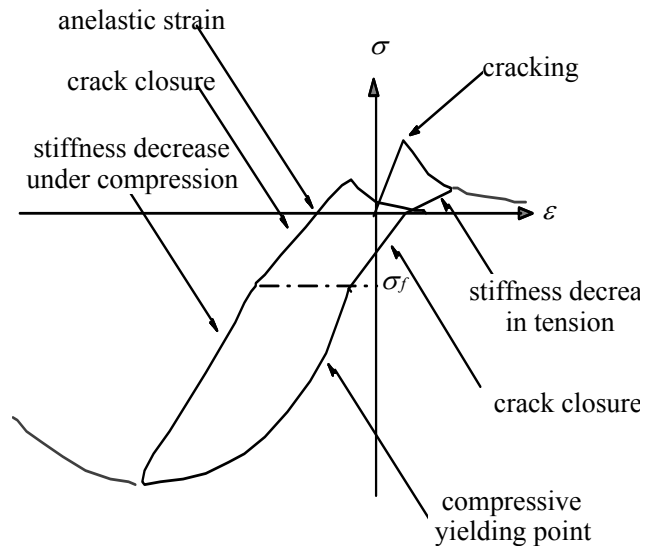


Figure 2. Effective panel area.

1.2 Mechanisms of bentonite hydration

Hydration of the bentonite will occur when water present in the soil underlying the GM-GCL migrates into the bentonite at the overlaps (Figure 1) and, then, flows laterally in the bentonite, thereby migrating laterally between the two geomembranes. Progressively, a growing area of the bentonite becomes hydrated. The analyses presented in this paper provide equations for quantifying the area of hydrated bentonite as a function of the following parameters: time, porosity and hydraulic conductivity of the bentonite, width of the overlap, distance between overlaps, and head difference that drives the migration of water.

In addition to the hydration mechanism described above, liquid leaking through defects in the upper geomembrane may contribute to the hydration of the bentonite layer. However, calculations performed by the authors, but not presented in this paper, show that hydration due to leakage through the upper geomembrane is negligible with respect to hydration through overlaps of the lower geomembrane. Therefore, the hydrated area can be calculated solely by consideration of liquid migration through the overlapped seams.

1.3 Driving head

The lateral migration of liquid is driven by the difference between the head at the bentonite hydration front and the head in the subgrade soil beneath the overlap. For unsaturated bentonite or soil, the head is negative, i.e. a suction. Therefore, the head difference, Δh , can be expressed as follows:

$$\Delta s = s_b - s_s \quad (1)$$

where s_b = matric suction in the bentonite at the hydration front; and s_s = matric suction of the soil.

1.4 Assumptions

In the analyses presented in Section 2, the bentonite layer thickness, t , is assumed to be uniform. The liquid migrating into the bentonite is assumed to be water or an aqueous solution with hydraulic properties similar to those of water. In particular, the liquid is assumed to be incompressible; therefore, mass conservation results in volume conservation.

2 THEORETICAL EVALUATION OF HYDRATED AREA

2.1 Phases of water migration

Three phases can be considered as migration of water from the underlying soil progresses in the bentonite layer (Figure 3). In each phase, the expression for the width of the hydrated area is different (Figure 4).

The first phase is when the water migration front is still in the overlap (Figure 3a). This phase is defined by:

$$B_1 \leq B_o \quad (2)$$

where B_1 = width of the fraction of the overlap that is hydrated at a given time during Phase 1.

In the first phase, the width of the hydrated area related to one panel (Figure 4a) is given by:

$$W_H = B_1 \quad (3)$$

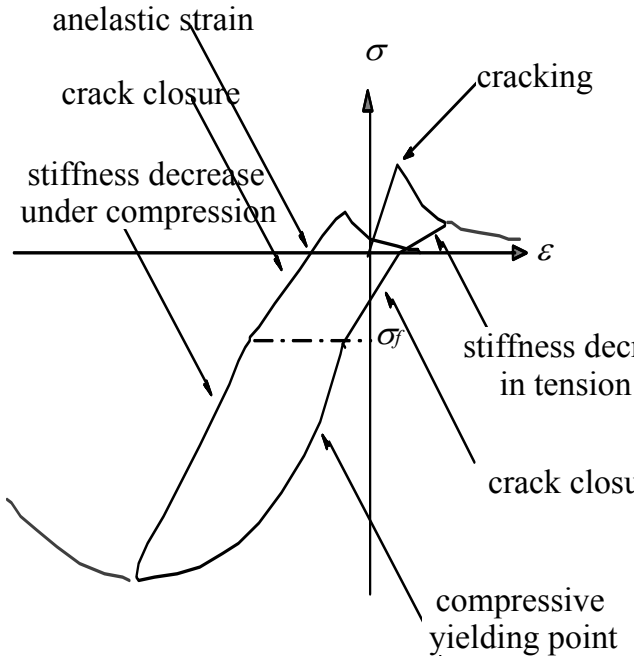


Figure 3. The three phases of liquid migration: (a) Phase 1; (b) Phase 2; (c) Phase 3.

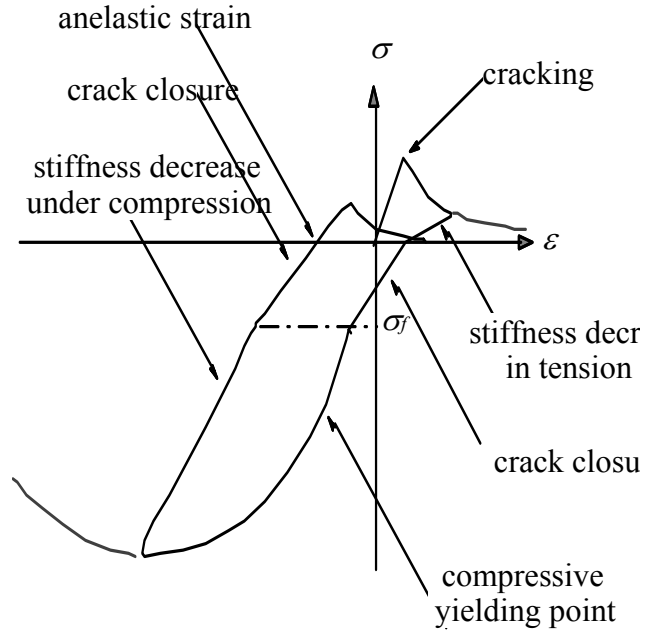


Figure 4. Width of hydrated area in each panel related to the liquid migration phase: (a) Phase 1; (b) Phase 2; (c) Phase 3.

The second phase starts when the migrating water has entirely hydrated the overlap, i.e. when:

$$B_1 = B_o \quad (4)$$

The second phase (Figure 3b) is defined by:

$$0 \leq B \leq B_o \quad (5)$$

where: B = distance reached by water beyond the overlap.

In the second phase, the width of the hydrated area related to one panel (Figure 4b) is given by:

$$W_H = B_o + B \quad (6)$$

The third phase starts when the width of the hydrated area is no longer governed by the overlap width, i.e. when:

$$B = B_o \quad (7)$$

From Equations 6 and 7, the width of the hydrated area at the beginning of Phase 3 is:

$$W_H = 2 B_o \quad (8)$$

The third phase (Figure 3c) is defined by:

$$B_o \leq B \leq \frac{W_P - B_o}{2} \quad (9)$$

In the third phase, the width of the hydrated area related to one panel (Figure 4c) is given by:

$$W_H = 2 B \quad (10)$$

The third phase ends when the bentonite layer is entirely hydrated, i.e. when the width of the hydrated area is equal to the effective panel width:

$$W_H = 2 B = W_P - B_o \quad (11)$$

hence:

$$B = \frac{W_P - B_o}{2} \quad (12)$$

2.2 Definition of the relative hydrated area

Overlaps are present at both sides and at both ends of each GCL panel. The hydration of a given panel proceeds simultaneously from both sides and both ends of the panel. It is assumed that, at the corners of the panel, the width of the hydrated area remains equal to W_H , as it is along the panels, in spite of the fact that, at the corners, water migrates from both the overlap at the panel side and the overlap at the end of the panel (Figure 5). In other words, it is assumed that the panel area that is not hydrated (referred to as the dry area) is perfectly rectangular (i.e. with right angles, not with rounded corners).

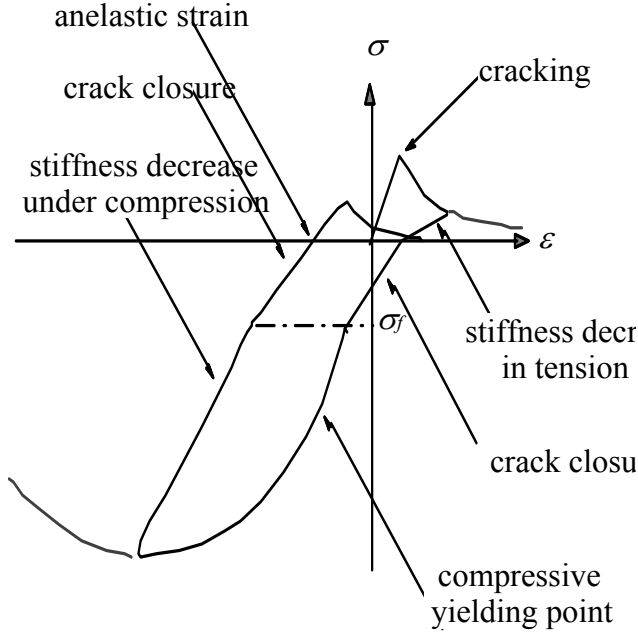


Figure 5. Rectangular shape of the dry area.

Based upon the assumption of a rectangular area, the hydrated area of a panel, A_H , is:

$$A_H = A_P - A_D \quad (13)$$

where: A_P = effective panel area; and A_D = dry area.

The effective panel area (Figures 2 and 5) is:

$$A_P = (W_P - B_o)(L_P - B_o) \quad (14)$$

The dry area (Figure 5) is:

$$A_D = (W_P - B_o - W_H)(L_P - B_o - W_H) \quad (15)$$

Combining Equations 13 to 15 gives the hydrated area of a panel as follows:

$$A_H = W_H(W_P + L_P - 2B_o) - W_H^2 \quad (16)$$

The relative hydrated area is defined as the ratio between the hydrated area and the effective panel area:

$$R_{HA} = \frac{A_H}{A_P} \quad (17)$$

Combining Equations 14, 16 and 17 gives:

$$R_{HA} = \frac{W_H}{W_P - B_o} + \frac{W_H}{L_P - B_o} - \left(\frac{W_H}{W_P - B_o} \right) \left(\frac{W_H}{L_P - B_o} \right) \quad (18)$$

Equation 18 is valid for all three phases of liquid migration, but the value of W_H depends on the phase, as indicated in Section 2.1. The value of W_H is given by Equation 3 for Phase 1, Equation 6 for Phase 2 and Equation 10 for Phase 3. In particular, at the end of Phase 3, Equations 12 and 18 give:

$$R_{HA} = 1.00 = 100\% \quad (19)$$

Also, if L_P is very large compared to W_P , Equation 18 tends to the following equation, which is obviously correct:

$$R_{HA} = \frac{W_H}{W_P - B_o} \quad (20)$$

2.3 Analysis of water migration

2.3.1 Assumption

It is assumed that water migration occurs in the direction perpendicular to the edge or end of panel. This is true everywhere except in corners. Since panel length is large compared with panel width, the approximation that results from this assumption is deemed acceptable.

2.3.2 Phase 1

During Phase 1, Darcy's equation can be written as follows:

$$Q/L = k i_1 (A/L) \quad (21)$$

where: Q/L = rate of liquid migration per unit length perpendicular to the plane of Figure 1; k = hydraulic conductivity of the hydrated bentonite (hereafter referred to as "hydraulic conductivity of the bentonite"); i_1 = hydraulic gradient in Phase 1; and A/L = cross-sectional area through which liquid is migrating per unit length perpendicular to the plane of Figure 1, i.e.:

$$A/L = t \quad (22)$$

where t is the thickness of the bentonite layer.

At a given time, \hat{t} , the hydraulic gradient, i_1 , is given by:

$$i_1 = \frac{\Delta h}{B_1} \quad (23)$$

Combining Equations 21 to 23 gives:

$$Q/L = \frac{k t \Delta h}{B_1} \quad (24)$$

At a given time, \hat{t} , the volume of liquid per unit length perpendicular to the plane of Figure 1 is:

$$V/L = n t B_1 \quad (25)$$

where n is the effective porosity of the bentonite, i.e. the ratio between the volume of water in hydrated bentonite and the total volume of hydrated bentonite.

Since the rate of liquid migration, Q , is the derivative of the volume with respect to time, volume conservation is expressed as follows, based on Equation 25:

$$Q/L = \frac{1}{L} \frac{dV}{d\hat{t}} = n t \frac{dB_1}{d\hat{t}} \quad (26)$$

Eliminating Q/L between Equations 24 and 26 gives:

$$d\hat{t} = \frac{n}{k \Delta h} B_1 dB_1 \quad (27)$$

Integration of Equation 27 (with $\hat{t} = 0$ for $B_1 = 0$) gives:

$$\hat{t}_1 = \frac{n}{2k\Delta h} B_1^2 \quad (28)$$

2.3.3 Interphase 1-2

The end of Phase 1, which is also the beginning of Phase 2, occurs when $B_l = B_o$, i.e. at time \hat{t}_{1-2} given by the following equation derived from Equation 28:

$$\hat{t}_{1-2} = \frac{n}{2k\Delta h} B_o^2 \quad (29)$$

2.3.4 Phases 2 and 3

When the migrating water reaches the end of the overlap, it bifurcates, i.e. the flow is shared between two GCL panels. The total bentonite thickness available for flow is t in the overlap and $2t$ after the overlap. Due to volume conservation, the flow rate is the same in the overlap and in the total of the two sections of length B , hence, based on Darcy's equation:

$$\frac{Q}{L} = k i_o \frac{A_o}{L} = k i_e \frac{A_e}{L} \quad (30)$$

where: i_o = hydraulic gradient in the overlap; i_e = hydraulic gradient in the bentonite section hydrated beyond the overlap; A_o/L = cross-sectional area through which liquid is migrating in the overlap per unit length perpendicular to the plane of Figure 1; and A_e/L = cross-sectional area through which liquid is migrating beyond the overlap per unit length perpendicular to the plane of Figure 1.

The total bentonite thickness available for flow is t for the portion of flow in the overlap, and $2t$ after the overlap, hence:

$$\frac{A_o}{L} = t \quad (31)$$

$$\frac{A_e}{L} = 2t \quad (32)$$

The hydraulic gradient is defined as the ratio between head loss and flow length, hence:

$$i_o = \frac{\Delta h_o}{B_o} \quad (33)$$

$$i_e = \frac{\Delta h_e}{B} \quad (34)$$

where: Δh_o = head loss in the overlap; and Δh_e = head loss in the bentonite section hydrated beyond the overlap.

The following relationship exists between the unknown head losses Δh_o and Δh_e and the known head difference, Δh :

$$\Delta h_o + \Delta h_e = \Delta h \quad (35)$$

Combining Equations 33 to 35 gives:

$$i_o = 2i_e = \frac{2\Delta h}{B + 2B_o} \quad (36)$$

Combining Equations 30, 32 and 36 gives:

$$\frac{Q}{L} = \frac{2k\Delta h}{B + 2B_o} \quad (37)$$

During Phases 2 and 3, the change in liquid volume stored in the bentonite layer is expressed by:

$$dV = 2ntLdB \quad (38)$$

Since the rate of liquid migration, Q , is the derivative of the volume with respect to time, volume conservation is expressed as follows, based on Equation 38:

$$Q = \frac{dV}{dt} = 2nt \frac{dB}{d\hat{t}} \quad (39)$$

Combining Equations 37, 38 and 39 gives:

$$\frac{2k\Delta h}{B + 2B_o} = 2nt \frac{dB}{d\hat{t}} \quad (40)$$

hence:

$$d\hat{t} = \frac{n}{k\Delta h} \frac{(B + 2B_o)dB}{d\hat{t}} \quad (41)$$

Integration of Equation 41 (with $\hat{t} = \hat{t}_{k-2}$ for $B = 0$), and using the notation $\hat{t} = \hat{t}_2$ for Phase 2 and $\hat{t} = \hat{t}_3$ for Phase 3, gives:

$$\hat{t}_2 = \hat{t}_3 = \hat{t}_{1-2} + \frac{nB^2}{k\Delta h} \left(\frac{1}{2} + \frac{2B_o}{B} \right) \quad (42)$$

Combining Equations 29 and 42 gives:

$$\hat{t}_2 = \hat{t}_3 = \frac{n}{2k\Delta h} \left(B_o^2 + B^2 + 4BB_o \right) \quad (43)$$

2.3.5 Interphase 2-3

For the limit case between the second and third period, combining Equations 7 and 43 gives:

$$\hat{t}_{2-3} = 6\hat{t}_{1-2} = \frac{3nB_o^2}{k\Delta h} \quad (44)$$

2.3.6 Limit case at the end of Phase 3

For the limit case at the end of the third phase, i.e. when the entire GCL area is hydrated, combining Equations 11 and 43 gives:

$$\hat{t}_{HYDR} = \frac{n}{8k\Delta h} \left(W_P^2 + 6W_P B_o - 3B_o^2 \right) \quad (45)$$

where \hat{t}_{HYDR} is the time at which the entire bentonite layer is hydrated, which marks the end of Phase 3.

2.3.7 General comment

Equations 28, 29, 43, 44, and 45 show that the time required for the liquid to reach a certain distance is independent of the bentonite layer thickness. However, this result exists only because the thickness of the bentonite layer is assumed to be uniform.

2.4 Calculation of relative hydrated area

The equations presented in Section 2.3 give the time required for the hydration front to reach a certain distance from the edge of the panel. These equations can be combined with equations presented in Sections 2.1 and 2.2 to obtain the relative hydrated area as a function of time.

2.4.1 Phase 1

Combining Equations 3, 18 and 28 gives:

$$R_{HA} = \sqrt{\frac{2k\hat{t}\Delta h}{n} \left(\frac{1}{W_P - B_o} + \frac{1}{L_P - B_o} \right)} - \frac{2k\hat{t}\Delta h}{n(W_P - B_o)(L_P - B_o)} \quad (46)$$

2.4.2 Phases 2 and 3

Equation 43 can be written as follows:

$$B^2 + 4 B B_o + B_o^2 - \frac{2 k t \Delta h}{n} = 0 \quad (47)$$

Equation 47 is a quadratic equation for the variable B . The positive solution of this equation is:

$$B = \sqrt{3 B_o^2 + \frac{2 k \hat{t} \Delta h}{n}} - 2 B_o \quad (48)$$

Since Equation 48 was derived from Equation 43, it is valid only for the second and the third phases. Combining Equations 6, 18 and 48 gives the following equation, which is valid only for the second phase:

$$R_{HA} = \left(\sqrt{3 B_o^2 + \frac{2 k \hat{t} \Delta h}{n}} - B_o \right) \left(\frac{1}{W_P - B_o} + \frac{1}{L_P - B_o} \right) - \frac{\left(\sqrt{3 B_o^2 + \frac{2 k \hat{t} \Delta h}{n}} - B_o \right)^2}{(W_P - B_o)(L_P - B_o)} \quad (49)$$

Combining Equations 10, 18 and 48 gives the following equation, which is valid only for the third phase:

$$R_{HA} = \left(2 \sqrt{3 B_o^2 + \frac{2 k \hat{t} \Delta h}{n}} - 4 B_o \right) \left(\frac{1}{W_P - B_o} + \frac{1}{L_P - B_o} \right) - \frac{\left(2 \sqrt{3 B_o^2 + \frac{2 k \hat{t} \Delta h}{n}} - 4 B_o \right)^2}{(W_P - B_o)(L_P - B_o)} \quad (50)$$

If B_o is negligible with respect to W_P and W_P is negligible with respect to L_P , Equation 50 gives the following upper boundary for the relative hydrated area, valid only for Phase 3:

$$R_{HA} \leq \frac{1}{W_P} \sqrt{\frac{2 k \hat{t} \Delta h}{n}} \quad (51)$$

3 PARAMETRIC STUDY

3.1 Parameters

3.1.1 Overview of the parameters

Based on Equations 46, 49 and 50, the rate at which a bentonite layer encapsulated between two geomembranes becomes hydrated depends of the following parameters: the length, L_P , and width, W_P , of the panels; the overlap width, B_o ; the porosity, n , and the hydraulic conductivity, k , of the bentonite; and the matric suctions that govern the head difference, Δh . For all cases considered in the parametric study, the panel width, W_P , is 5.2 m, and the panel length, L_P , is 61 m. A constant value of 0.4 has been assumed for the effective porosity of the bentonite.

The three parameters used as variables in the parametric study (k , Δh and B_o) are the parameters that are most likely to vary for different applications of encapsulated GCLs. These three parameters are discussed below.

3.1.2 Hydraulic conductivity of the bentonite

The hydraulic conductivity of the bentonite depends on the degree of saturation and the overburden pressure. The hydraulic conductivity used in the parametric study for the hydrated bentonite is the hydraulic conductivity of the saturated bentonite. This is conservative (with respect to the rate of hydration) because the hydrated bentonite is not completely saturated and the hydraulic conductivity of unsaturated bentonite is less than, or equal to (but never greater than), the hydraulic conductivity of saturated bentonite. The hydraulic conductivity of bentonite decreases with increasing values of the overburden pressure. Hydraulic conductivities that correspond to overburden pressures of 5 kPa and 500 kPa are used in the parametric study: 5 kPa is representative of a landfill cover, and 500 kPa is representative of a landfill liner overlain by approximately 50 m of waste. The following values of hydraulic conductivity of saturated bentonite were selected based upon data developed by Daniel (1996): 5×10^{-11} m/s under 5 kPa and 1×10^{-12} m/s under 500 kPa.

3.1.3 Matric suction

As shown by Equation 1, the head difference that drives water migration depends on both the bentonite matric suction and the subgrade matric suction. Two values of the matric suction in the bentonite at the hydration front are used in the parametric study: $s_b = 3$ m, as recommended by Thiel et al. (2001), and $s_b = 10$ m, to evaluate the impact of a more conservative assumption. Subgrade matric suction typically varies between 0 m (coarse grained soils or saturated fine grained soils) and 1 m (dry fine grained soils), according to Estornell and Daniel (1992). Therefore, values of 0 m and 1 m were used in the parametric study.

3.1.4 Overlap width

Nominal overlaps between 0.15 m and 0.3 m are typically used in the field at GCL seams. Therefore, overlaps of 0.15 m and 0.3 m were used in the parametric study.

3.2 Results of the parametric study

3.2.1 Influence of suction and hydraulic conductivity

Equations 28, 29, 43, 44, and 45 show that the time required for the liquid to reach a certain distance (hence the time required to reach any given relative hydrated area, such as 50%) is inversely proportional to k and Δh . This is illustrated in Table 1 that gives the time required for hydration of the entire bentonite panel in the case of a 0.15 m overlap, with the values indicated in Section 3.1.1 for the other parameters (L_P , W_P and n). It appears in Table 1 that the bentonite hydraulic conductivity has a large influence on the rate of hydration. Thus, hydration is 50 times faster in the case representative of a landfill cover ($k = 5 \times 10^{-11}$ m/s under 5 kPa) than in the case representative of a landfill liner ($k = 1 \times 10^{-12}$ m/s under 500 kPa), because the bentonite hydraulic conductivity is 50 times greater under a 5 kPa overburden pressure than under a 500 kPa overburden pressure.

Table 1. Time required for hydrating the entire panel.

Bentonite hydraulic conductivity	$s_b = 3$ m		$s_b = 10$ m	
	$s_s = 1$ m $\Delta h = 2$ m	$s_s = 0$ m $\Delta h = 3$ m	$s_s = 1$ m $\Delta h = 9$ m	$s_s = 0$ m $\Delta h = 10$ m
1×10^{-12} m/s	25,000 yrs	17,000 yrs	5500 yrs	5000 yrs
5×10^{-11} m/s	500 yrs	330 yrs	110 yrs	100 yrs

Based on Equation 51, the times given in Table 1 should be divided by 4 to obtain an approximate value of the time required for reaching a relative hydrated area of 50%.

Table 1 shows that the subgrade matric suction, s_s , varies in a range that is too narrow to have a marked influence on the hydrated area if the matric suction in the bentonite at the hydration front, s_b , is equal to or greater than 3 m. Table 1 also shows that the assumed value of the matric suction in the bentonite at the hydration front has a significant impact on the calculated value of the time required for hydration

3.2.2 Influence of overlap width

Figure 6 illustrates the influence of the overlap width (0.15 m and 0.3 m) for the case of a landfill liner (i.e. bentonite hydraulic conductivity of 1×10^{-12} m/s, which corresponds to an overburden pressure of 500 kPa), with a head difference of 3 m. It appears in Figure 6 that the impact of overlap width on hydrated area does not follow a simple pattern. To interpret Figure 6, it is useful to calculate the transition times using Equations 29 and 44. The following values are obtained for the 0.15 m overlap (dashed curve in Figure 6):

$$\hat{t}_{1-2} = 48 \text{ years} \quad \text{and} \quad \hat{t}_{2-3} = 285 \text{ years}$$

and the following values for the 0.3 m overlap (solid curve in Figure 6):

$$\hat{t}_{1-2} = 190 \text{ years} \quad \text{and} \quad \hat{t}_{2-3} = 1142 \text{ years}$$

For the first 48 years, the 0.15 m wide overlap and the 0.3 m wide overlap correspond approximately to the same hydrated area (the relative hydrated area is 3.2% with the 0.15 m wide overlap and 3.3% with the 0.3 m wide overlap at 48 years). Then, between 48 years and 358 years, a larger hydrated area is achieved with the 0.3 m wide overlap than with the 0.15 m wide overlap. Finally, beyond 358 years, a larger hydrated area is achieved with the 0.15 m wide overlap than with the 0.3 m wide overlap. This complex pattern is due to the three different phases of hydration of an encapsulated GCL. During phase 1, when the first section of the overlap is becoming hydrated, the rate of hydration is at its quickest because the thickness of bentonite available for flow is the smallest. During Phase 2, the rate of hydration decreases because the thickness of bentonite available for flow doubles. During Phase 2, the “virgin” hydration front advances in only one direction because, in the other direction, the hydration front is “doubling-back” over the already-hydrated seam. During Phase 3, the rate of GCL hydration increases because the hydration front that doubled-back has advanced beyond the leading edge of the seam and the virgin hydration front is advancing on both sides of the overlap. These three phases of encapsulated GCL hydration are delineated by the inflection points in Figure 6. These points correspond to the values of \hat{t}_{12} and \hat{t}_{23} given above.

Figure 6 shows that the time required to reach a relative hydrated area of 12% is approximately 80% greater with an overlap width of 0.3 m than with an overlap of 0.15 m. This difference is large because, in this case, hydration is in Phase 2 with the 0.3 m overlap and in Phase 3 with the 0.15 m overlap. The difference is smaller (i.e. 15%) at 100% hydration as shown by using Equation 45 with $B_o = 0.15$ m and $B_o = 0.3$ m.

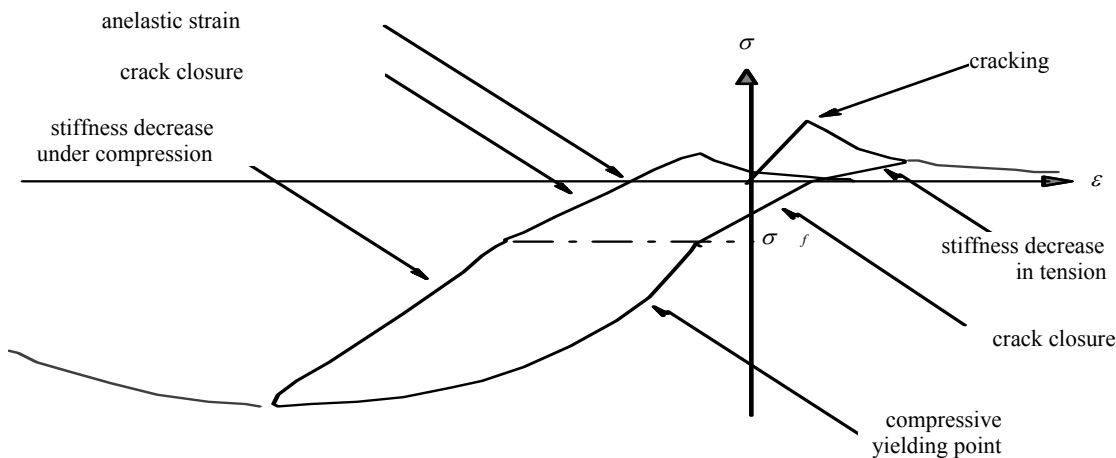


Figure 6. Influence of overlap width on hydrated area for a head difference of 3 m.

4 CONCLUSIONS

The equations presented in this paper make it possible to evaluate the area of hydrated bentonite in the case of a bentonite layer encapsulated between two geomembranes. The only hydration mechanism considered in this paper is by water from the ground migrating through overlaps of the lower geomembrane.

The main parameters that govern the hydrated area due to water migration through the overlaps in the lower geomembrane are: the hydraulic conductivity of the bentonite, the head difference that drives the migration of water, and the overlap width. A parametric study performed to evaluate the influence of these parameters on the extent of the hydrated area for a given time (or the time required to reach a certain relative hydrated area) showed the following.

The influence of the bentonite hydraulic conductivity is very large because the extent of the hydrated area is inversely proportional to the hydraulic conductivity, and because bentonite hydraulic conductivity can vary significantly depending on overburden pressure. Therefore, there is a large difference between landfill covers (low overburden pressure) and landfill liners (high overburden pressure).

The influence of suction in the bentonite at the hydration front can be large because the extent of the hydrated area is inversely proportional to the head difference (which is governed by suction). There is some uncertainty with this parameter, as little information is available on suction at the hydration front.

The influence of the overlap width is complex. Increasing the overlap width of the encapsulated GCL panels increases the rate at which the GCL becomes hydrated over short time periods and decreases the rate of hydration for longer time periods. The influence of overlap width is small compared to the influence of the two other parameters investigated, the bentonite hydraulic conductivity and the suction.

Considering the large influence of parameters on hydrated area, it is important to properly and conservatively select the parameter values used in design. Information provided in this paper can be used as guidance.

REFERENCES

- Daniel, D.E., 1996. Geosynthetic Clay Liners, Part Two: Hydraulic Properties. *Geotechnical Fabrics Report* 14, (5), June/July. 22-26.
- Estornell, P. & Daniel, D.E., 1992. Hydraulic Conductivity of Three Geosynthetic Clay Liners. *Journal of Geotechnical Engineering* 118, (10), 1592-1606.
- Thiel, R.S., Daniel, D.E., Erickson, R.B., Kavazanjian, E. & Giroud, J.P. 2001. The GSE GundSeal GCL Design Manual.